A Control Framework Definition to Overcome Position/Interaction Dynamics Uncertainties in Force-Controlled Tasks

Loris Roveda[1], Nicola Castaman[2,3], Paolo Franceschi[1], Stefano Ghidoni[2], Nicola Pedrocchi[1]

***Abstract*— Within the Industry 4.0 context, industrial robots need to show increasing autonomy. The manipulator has to be able to react to uncertainties/changes in the working environment, displaying a robust behavior. In this paper, a control framework is proposed to perform industrial interaction tasks in uncertain working scenes. The proposed methodology relies on two components: i) a 6D pose estimation algorithm aiming to recognize large and featureless parts; ii) a variable damping impedance controller (inner loop) enhanced by an adaptive saturation PI (outer loop) for high accuracy force control (*i.e.*, zero steady-state force error and force overshoots avoidance). The proposed methodology allows to be robust w.r.t. task uncertainties (*i.e.*, positioning errors and interaction dynamics). The proposed approach has been evaluated in an assembly task of a side-wall panel to be installed inside the aircraft cabin. As a test platform, the KUKA iiwa 14 R820 has been used together with the Microsoft Kinect 2.0 as RGB-D sensor. Experiments show the reliability in the 6D pose estimation and the high-performance in the force-tracking task, avoiding force overshoots while achieving the tracking of the reference force.**

I. Introduction

Considering the Industry 4.0 (I4.0) scenario, manipulators are taking in charge onerous and repetitive tasks [1] to relieve humans from mental and physical heavy operations [2]. A wide range of such applications can be classified as interaction tasks [3]: the manipulator has to interact with the surrounding environment to achieve its goals (*e.g.*, assembly tasks). While performing such applications, the manipulator has to be capable to sense the working scenario, identifying the components to be manipulated and controlling such interaction [4]. However, considering the I4.0 paradigm, the industrial plant (and, therefore, the manipulator working place) becomes a dynamic and flexible environment, allowing the reconfigurability of the cells to pander the production requirements [5]. In such a scenario, the capability of the robotic system to dynamically map the working place, identifying the proper actions to be executed, is mandatory. Moreover, the implemented control methodologies have to be robust in order to deal with uncertain interaction dynamics while achieving high performance.

The work has been developed within the project EURECA, funded from H2020 CleanSky 2 under grant agreement n. 738039.

[1] Loris Roveda, Paolo Franceschi and Nicola Pedrocchi are with the Institute of Intelligent Industrial Technologies and Systems for Advanced Manufacturing (STIIMA) of Italian National Research Council (CNR), via Corti, 12 - 20133 Milan, Italy nicola.pedrocchi@stima.cnr.it

[2] Nicola Castaman and Stefano Ghidoni are with Intelligent Autonomoud System Lab (IAS-Lab) of the University of Padova, Padova, Italy stefano.ghidoni@unipd.it

[3] Nicola Castaman is also with IT+Robotics srl, Vicenza, Italy nicola.castaman@it-robotics.it

A. 6D Pose Estimation

In order to obtain flexible autonomous robots, manipulating parts in unstructured environments, it is essential to exploit vision systems and computer vision algorithms to face with parts position uncertainty. Recognition and pose estimation algorithms are, therefore, used to identify an object and to estimate its 6D pose in the environment.

Most of the pose estimation methods proposed in the last decade are based on local features [6], [7] used on 2-dimensional images took from slightly different viewpoints [8]. Feature-based approaches are well suited for objects with a texture. Conversely, when dealing with object without texture, the performance of those algorithms would degrade significantly. To overcome this issue, alternative detection and pose estimation approaches based on the edges [9]–[11] were proposed. However, local features and edges on 2D images are not very reliable in case of changes in lighting or strong reflections.

Other popular approaches for recognition and 6D pose estimation are based on 3D Point Cloud and uses the 3D CAD model for object recognition and shape matching [12]. In such approaches there are different methods that use global descriptors or local descriptors [13]. Local descriptors are computed for individual points or around keypoints while global descriptors encode object geometry and are computed for the cluster that represents an object. However, also those methods rely on objects with strong visual features (*e.g.*, texture, complex shape, etc.).

Recent methods based on machine learning and CNNs can effectively face the problem of lacking visual features [14]. However, machine learning approaches need large datasets

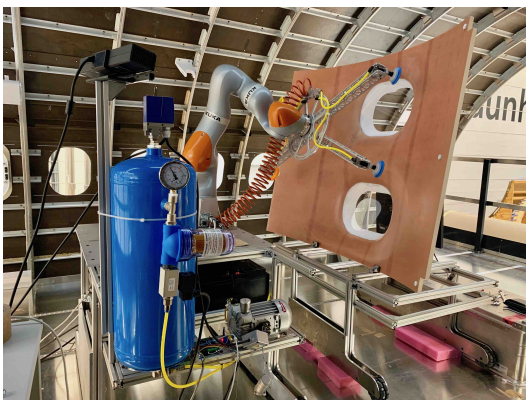

Fig. 1: Experimental setup: the KUKA iiwa 14 R820 and the Microsoft Kinect 2.0 are used to assembly a sidewall panel.

with thousands of labeled training samples, resulting in a significant amount of time for each new object.

B. Force-Tracking Control

The need to control the interaction between the robot and the environment is required in many industrial applications [15]. In order to deal with (partially) unknown environments, impedance [16] based controllers can be adopted to implement a required robot dynamics, while allowing the tracking of a specific position/force. Control methodologies have been developed in order to achieve high performance during the interaction control applications, exploiting (a) Setpoint Deformation (SD) methodologies [17]–[19] and Variable Impedance Adaptation (VIA) [20]–[22].

SD algorithms aim to deform the impedance control setpoint to achieve position/force tracking. Such deformation is often based on the estimation of the interaction environment stiffness [17]. Many different approaches have been developed, from simple proportional gain controllers to more advanced algorithms, involving *e.g.*, machine learning methodologies [18] or non-contact to contact transients control [19]. VIA methods aim to adapt the impedance parameters (*i.e.*, damping and/or stiffness parameters) during the interaction execution. The developed methodologies relies only on the force feedback to tune the impedance control parameters in order to achieve the target interaction force. Commonly, SD approaches maintain a constant dynamic behavior of the robot (resulting in limited controllers bandwidth). VIA approaches adapt the bandwidth of the controllers on the basis of the measured interaction, however, being affected by force overshoots and steady-state force errors. In fact, even if some approaches consider *energy tanks* and/or *task energy* to guarantee the passivity (*i.e.*, the stability) of the controlled robot [23], such approaches are not considering the force overshoot issue in the controller design.

Few approaches are considering the impact issue. [24] developed a hybrid position-force controller exploiting multiple 1D-distance measurement radars to detect the interaction environment position and switching control mode. However, its validation is only available in simulation. Moreover, the used 1D-distance measurement radars work in a free-occlusions scenario. [25] developed instead an SD approach exploiting the estimation of the interaction environment stiffness. However, such estimation requires the modeling of the environment and a more complex implementation to tune the different parts of the algorithm.

C. Paper Contribution

The aim of the proposed paper is to overcome the above discussed difficulties in autonomous interaction tasks (*i.e.*, parts positioning and interaction dynamics uncertainties), effectively combining vision algorithms and interaction control. The works in the field commonly concentrate only on the vision part [26] or on the control part [27]. Some approaches are effectively combining vision techniques and interaction control, however, without considering force overshoot issues and implementing simple state-of-the-art controller [28]. The proposed approach, therefore, aims to combine the advantages of both the vision and advanced control techniques. In particular, two main components are proposed: i) a 6D pose estimation algorithm, and ii) a variable damping impedance controller (inner loop) enhanced by an adaptive saturation PI (outer loop) for force-tracking performance. i) exploits the 6D pose estimation algorithm, so that large and textureless parts can be identified in the industrial environment, providing the initial robot positioning. ii) exploits the proposed force-tracking algorithm, so that high accuracy in force control task (*i.e.*, zero steady-state force error and force overshoots avoidance) is achieved, without any knowledge of the interaction dynamics (*i.e.*, no need to online estimate the part/environment compliance such as in [25]). The force-tracking algorithm combines a variable damping impedance controller (to achieve an over-damped robot behavior) with an adaptive saturation PI force controller (to avoid force overshoots while tracking the reference force). The developed methodology has been evaluated in an assembly task involving a sidewall panel (*i.e.*, a big-size compliant part) in the aerospace industry context of the H2020 CleanSky 2 EURECA project [29]. Robot and part are positioned inside the cluttered environment with positioning (no calibrated positions) and interaction dynamics uncertainties (unknown interaction dynamics). As a test platform, the KUKA iiwa 14 R820 has been used together with the Microsoft Kinect 2.0 RGB-D sensor as depicted in Figure 1. Results show the capabilities of the proposed approach to achieve high accuracy in the part pose estimation and in the force-tracking performance in a real industrial task execution, involving a compliant big-size part with complex assembly features.

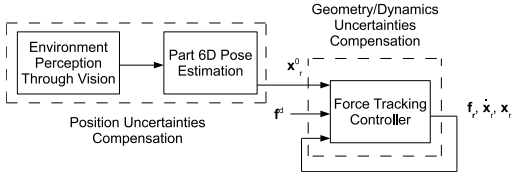

Fig. 2: Uncertainties compensation control framework involving the 6D pose estimation and the force-tracking controller.

II. Problem Formulation

The proposed control framework is shown in Figure 2, highlighting the proposed 6D pose estimation algorithm and the force-tracking controller. The 6D pose estimation algorithm provides the robot with the initial pose to start the task, while the force-tracking controller enhances the force control performance.

A. 6D Pose Estimation

The proposed recognition and 6D pose estimation approach adopts a CAD-based model strategy. In general, the 3D CAD models of parts are easy to obtain, and CAD-based methods are robust in scenarios where lighting changes significantly and are flexible to be used in industrial domain.

The proposed approach aims to face two issues that most often characterize industrial parts w.r.t. everyday objects:

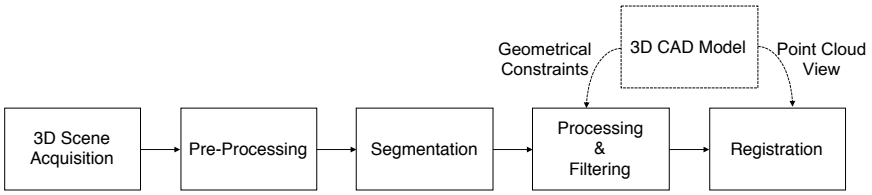

Fig. 3: The pipeline of the proposed 6D pose estimation system.

- *Textureless*: indeed most industrial parts are metallic or textureless and have simple shapes;
- *Large Dimension*: industrial parts could have large dimension, observed from only one point of view, and not always completely visible from the camera.

The pipeline of the proposed method is shown in Figure 3, highlighting the three main steps: i) pre-proccesing and segmentation, ii) processing and filtering, and iii) 6D pose estimation.

1) Pre-Processing and Segmentation: To efficiently and reliably implement the 6D pose estimation, a pre-processing phase is performed to filter out the noise and reduce the number of points:

- *Noise Removal*: A statistical outlier removal filter [30] is applied to reduce the noise from the sensor in the acquired point cloud.
- *Downsample*: Point clouds has a large number of points that increase the computational cost. Voxel Grid filter is used to reduce number of points while preserving the precision in pose estimation.

Segmentation allows to subdivide the scene into clusters that represent a part each one. The proposed approach exploits Region Growing [31] segmentation algorithm. Such algorithm merges the points that are close enough in terms of the smoothness constraint so each extracted cluster is a set of points that are considered to be a part of the same smooth surface.

2) Processing and Filtering: Geometrical constraints are used to filter out the clusters that are incompatible with the looking for part. First, the Oriented Bounding Box (OBB) is computed for each cluster. The OBB is the smallest bounding box that contain a set of points. OBB dimensions are compared with the real ones from the 3D CAD of the part. In the case that the dimensions are comparable within a margin of error, corresponding cluster is selected as a guess, otherwise the cluster is rejected.

3) 6D Pose Estimation: Considering that the part is visible from only one side, from the 3D CAD model is extracted the point cloud of the corresponding view. Such point cloud is used as a mask in order to perform the registration with the extracted clusters. The computed oriented bounding box provide also a pose that is used as initial guess to perform a pre-alignement of the part mask over each extracted cluster. Iterative Closest Point (ICP) [32] is then used to refine the alignment and improve the estimation accuracy, and the distance between the mask and the cluster is computed. Finally the cluster with lower distance is selected as the reference.

B. Force-Tracking Controller

The proposed force-tracking controller is defined by two main components: i) an inner variable damping impedance controller, and ii) an outer force-tracking controller (Figure 4). While in i) the impedance control damping is updated on the basis of the reference force function achieving an over-damped interaction dynamics, in ii) a PI force-tracking controller is designed with adaptive saturation (to avoid force overshoots while achieving a zero steady-state force error) and anti-windup loop.

General Notation

$\mathbf{M}_r$, $\mathbf{D}_r$, $\mathbf{K}_r$	: mass, damping and stiffness Cartesian impedance matrices
$\mathbf{f}_r$	: external wrench vector
$\Delta\mathbf{x}_r = \mathbf{x}_r - \mathbf{x}_r^d$	: where $\mathbf{x}_r$ is the Cartesian robot positioning and $\mathbf{x}_r^d$ is the impedance control setpoint
$\mathbf{K}_p$, $\mathbf{K}_i$	: proportional and integral control gain diagonal and positive matrices
$\mathbf{f}^d$, $\mathbf{f}_f^d$	: step reference and filtered force
$\mathbf{e}_f$, $\int \mathbf{e}_f$	: force error ($\mathbf{e}_f = \mathbf{f}_f^d - \mathbf{f}_r$) and its integral

1) Cartesian Impedance Control: In order to implement the proposed force-tracking controller, the inner Cartesian impedance control has to be designed [16]:

$$\mathbf{M}_r \ddot{\mathbf{x}}_r + \mathbf{D}_r \dot{\mathbf{x}}_r + \mathbf{K}_r \Delta\mathbf{x}_r = \mathbf{f}_r. \tag{1}$$

Impedance control receives the initial force-tracking task position $\mathbf{x}_r^0$ from the 6D pose estimation algorithm in order to compensate for (macro) positioning errors.

On top of the impedance controller, the outer force-tracking control (to update the impedance control setpoint $\mathbf{x}_r^d$) and the variable damping law (to update the impedance control damping parameters $\mathbf{D}_r$) are implemented.

Remark. Impedance control damping can be calculated as follows $\mathbf{D}_r = 2\sqrt{\mathbf{M}_r\mathbf{K}_r}\mathbf{h}_r$, where $\mathbf{h}_r$ the damping ratio matrix.

2) Adaptive Saturation PI Force-Tracking Controller: In order to achieve a zero steady-state force error while avoiding force overshoots, a PI force-tracking controller with adaptive saturation and anti-windup is designed. Such outer controller allows to update the impedance control setpoint $\mathbf{x}_r^d$. The PI force-tracking control with anti-windup allows to calculate the updated not-saturated reference position $\mathbf{x}_{PI}$:

$$\mathbf{x}_{PI} = \mathbf{K}_p\mathbf{e}_f + \mathbf{K}_i \int \mathbf{e}_f + \mathbf{AWU}. \tag{2}$$

AWU is the anti-windup term. $\mathbf{K}_p$ and $\mathbf{K}_i$ are the proportional and integral control gain matrices. The saturation has to be

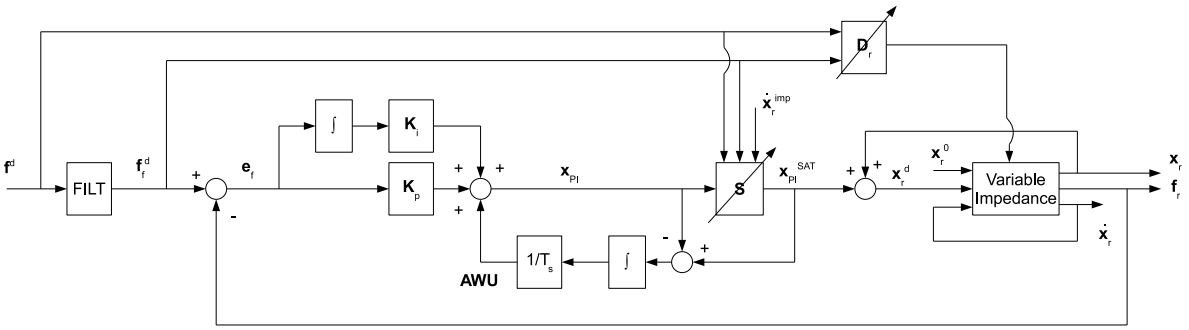

Fig. 4: Proposed control schema highlighting the inner variable impedance control and the outer force-tracking control.

applied to such reference position $\mathbf{x}_{PI}$ in order to calculate the saturated reference position $\mathbf{x}_{PI}^{sat}$:

$$\begin{aligned} \mathbf{x}_{PI}^{sat}(i) &= \mathbf{x}_{PI}(i) \ if \ \ |\mathbf{x}_{PI}(i)| \leq \mathbf{S}(i) \\ \mathbf{x}_{PI}^{sat}(i) &= sign(\mathbf{x}_{PI}(i))\mathbf{S}(\mathbf{i}) \ if \ \ |\mathbf{x}_{PI}(i)| > \mathbf{S}(i), \end{aligned} \tag{3}$$

where i denotes the i^{th} Degree of Freedom (DoF). The proposed approach defines the saturation $\mathbf{S}$, to achieve zero steady-state force error and the avoidance of force overshoots, by two contributions:

$$\mathbf{S} = \mathbf{FT} - \mathbf{IMP}. \tag{4}$$

The first term $\mathbf{FT}$ allows to achieve the zero steady state force error and it is defined as follows:

$$\mathbf{FT}(i) = \mathbf{K}_r(i,i)^{-1}\left(2\mathbf{f}^d(i) - \mathbf{f}_f^d(i)\right), \tag{5}$$

where i denotes the i^{th} DoF. When time is zero $\mathbf{FT}(i) = 2\mathbf{f}^d(i)$, while at the steady-state t_{ss} $\mathbf{FT}(i) = \mathbf{f}^d(i)$, having a decreasing saturation from the first contact instant to the steady-state. It means that the manipulator is allowed to have initially a faster dynamics to achieve the target force $\mathbf{f}^d$.
The second term $\mathbf{IMP}$ allows to reduce the saturation of the controller on the basis of the initial impact force. The resulting impact force can be estimated as follows [25]:

$$\mathbf{f}_{imp}(i) = \frac{(1+\lambda)\mathbf{M}_r(i,i)\dot{\mathbf{x}}_r^{imp}(i)}{dt_{imp}}, \tag{6}$$

where λ is the coefficient of restitution ($0 \leq \lambda \leq 1$) and dt_{imp} is the duration of the impact ($0 < dt_{imp} \leq 0.005$ $[s]$) [33]. $\dot{\mathbf{x}}_r^{imp}$ is the impact velocity of the robot with the environment.
On the basis of (6) it is possible to calculate $\mathbf{IMP}$:

$$\mathbf{IMP} = \mathbf{K}_r^{-1} diag\left(\mathbf{f}^d\right)^{-1} diag\left(\mathbf{f}^d - \mathbf{f}_f^d\right)\mathbf{f}_{imp}. \tag{7}$$

In such a way, since initially $\mathbf{f}_f^d = \mathbf{0}$ it results $\mathbf{IMP} = \mathbf{K}_r^{-1}\mathbf{f}_{imp}$, while at the steady-state since $\mathbf{f}_f^d = \mathbf{f}^d$ it results $\mathbf{IMP} = 0$. Therefore, such term reduce initially the saturation of the controller and it expires at the steady state.

The anti-windup term $\mathbf{AWU}$ in (2) is calculated as follows:

$$\mathbf{AWU} = \frac{\int(\mathbf{x}_{PI}^{sat} - \mathbf{x}_{PI})}{T_s}, \tag{8}$$

where T_s is the time constant of the anti-windup loop.

The impedance control setpoint $\mathbf{x}_r^d$ is updated as follows:

$$\mathbf{x}_r^d = \mathbf{x}_r + \mathbf{x}_{PI}^{sat}. \tag{9}$$

Remark. Force control is activated when reference force component is > 5 N.

3) Variable Damping Law: The damping parameters of the impedance control are tuned to have a fast dynamics of the controlled manipulator starting the force-tracking task, while achieving an over-damped behavior of the interaction dynamics as soon as the target force is obtained, aiming to avoid force overshoots. Therefore, the damping matrix $\mathbf{D}_r$ is updated on the basis of the following linear law:

$$\mathbf{D}_r(i,i) = diag(\mathbf{f}_f^d(i))^{-1} diag(\mathbf{f}_f^d(i))\mathbf{m}_h(i,i) + \mathbf{q}_h(i,i), \tag{10}$$

where $\mathbf{m}_h$ and $\mathbf{q}_h$ are the diagonal matrices of coefficients of the linear law and can be calculated by substituting the following conditions in (10):

$$\begin{aligned} \mathbf{D}_r(i,i) &= \mathbf{D}_r^i(i,i) \ with \ \mathbf{f}_f^d(i) = \mathbf{0} \\ \mathbf{D}_r(i,i) &= \mathbf{D}_r^f(i,i) \ with \ \mathbf{f}_f^d(i) = \mathbf{f}^d(i), \end{aligned} \tag{11}$$

where $\mathbf{D}_r^i$ is the initial damping matrix and $\mathbf{D}_r^f$ is the final damping matrix. In particular, $\mathbf{D}_r^i$ is defined in order to have a low-damped robot behavior, while $\mathbf{D}_r^f$ to achieve an over-damped robot behavior.

III. Experimental Evaluation

A. Setup Description

1) Task Description: To validate the proposed approach, an assembly task of a sidewall panel in the aerospace industry scenario has been considered (Figure 1). Two main phases are defined: i) a grasping phase, and ii) an installation phase. The task shows the typical issues related to real industrial applications: uncertainties on the relative robot-part positioning and unknown interaction dynamics.

2) Hardware Description: The KUKA iiwa 14 R820 has been used as a validation platform. The employed vision system is a Kinect 2.0, an RGB-D camera based on Time-of-Flight (ToF) technology. This sensor acquires a 512×424 depth map and a 1920×1080 color image at 30 fps. This new version of the sensor is two times more accurate in the near range and even ten times more accurate after 6 meters of distance w.r.t. its predecessor Kinect 1.0 [34]. The vision system is in eye-to-hand configuration (*i.e.*,

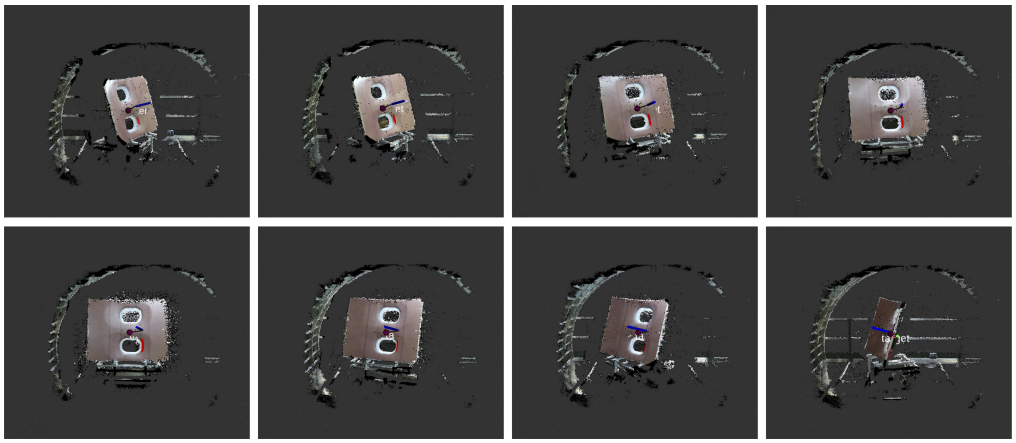

Fig. 5: Examples of pose estimation experiments performed on a sidewall panel in the project demonstrator at Fraunhofer IFAM. From left to right and top to bottom: $-60°$, $-45°$, $-30°$, $-15°$, $0°$, $20°$, $40°$, $70°$.

the camera is rigidly placed w.r.t. the robot arm base - Figure 1). In general, computer vision algorithms determine where an object is w.r.t. the camera coordinate system, but the robot arm does not know how to reach the part to grasp it. Therefore, to move the robot arm to the estimated grasping point, the transformation matrix from the robot base frame to the vision system frame has to be computed. The transformation matrix from the robot base frame to the end-effector frame is known through the robot kinematics, and the AprilTag fiducial marker system [35] is used to estimate the transformation matrix from the camera frame and the end-effector. Hand-eye calibration from Tsai [36] is used to estimate the transformation matrix between the robot base frame and the camera frame. A vacuum gripper is used to ensure the grasping, manipulation and installation of the part. The manipulator and the vision system are mounted on a carrier and the sidewall panel is positioned on another carrier, both positioned inside the working environment. The installation features are plastic snap fit fixing parts.

3) Software Description: The control schema described in Section II-B has been implemented on top of the KUKA iiwa low level joint position controller through its *FRI* (Fast Research Interface) control framework exploiting *ROS*. A control frequency of 200 Hz has been achieved. The estimated external wrench $\mathbf{f}_r$ from its internal joint torque sensors has been used as a feedback to the inner impedance controller and to the outer force-tracking controller.

The motion planning of the manipulator (to grasp and install the part) is online computed. Exploiting *MoveIt!*, the working scene is composed, including all the components (robot, parts, carriers, fuselage). The manipulator motion between grasping and installation phases is, therefore, computed to avoid any collision while positioning the part.

The control parameters have been imposed as follows. The reference step force $\mathbf{f}^d$ has been filtered at 0.65 Hz to calculate the filtered reference force $\mathbf{f}_f^d$. The impedance control stiffness $\mathbf{K}_r$ has been imposed equal to 300 N/m for the translational DoFs, and equal to 20 Nm/rad for rotational DoFs. The impedance control mass $\mathbf{M}_r$ has been imposed equal to 10 kg for the translational DoFs, and equal to 1 kgm^2 for rotational DoFs. $\mathbf{D}_r^i$ has been imposed to have a damping ration $\mathbf{h}_r^i(i,i) = 0.7$ for all the DoFs. $\mathbf{h}_r^f(i,i) = 25$ is imposed to achieve an over-damped interaction dynamics. λ parameter in (6) has been imposed equal to 2. dt_{imp} parameter in (6) has been imposed equal to 0.005 s. T_s parameter in (8) has been imposed equal to 0.1 s.

B. Sidewall Panel Pose Estimation

The developed 6D pose estimation pipeline has been evaluated in the sidewall panel pose estimation. The part has been positioned in different configurations w.r.t. the camera position. Figure 5 shows how the 6D pose estimation system is able to recognize and estimate the 6D pose of the side-wall panel rotated in different angles w.r.t. the camera mounted on the robot carrier. During experimental data acquisition, part rotation has been varied between $-70°$ and $70°$, while the position have been varied in a radius of 15 cm from a nominal position. Twelve different configurations were acquired and the 6D poses of the part have been manually labeled. Ten repetition of pose estimation have been performed for each part configuration. Object pose predictions with error in translation smaller than 2 cm and error in orientation smaller than $3°$ are assumed as correct identification. In the described experimental conditions, 6D pose estimation algorithm predict with a 100% success rate the sidewall panel 6D pose until $\pm 45°$ with a standard deviation of 1 millimeter in the measure of the same configuration. Performances instead decrease to 70% success rate until $\pm 70°$ and standard deviation increased to 3 millimeters.

C. Assembly Task Execution

The force-tracking controller has been evaluated in the assembly of the sidewall part (grasping and installation). The proposed force-tracking controller has been compared with a standard controller: a constant-damping impedance controller with non-saturated PI (control parameters have been imposed as in Section III-A.3, with constant damping equal to $\mathbf{D}_r^i$). Considering grasping phase, exploiting the identified part location, the robot is positioned to start the grasping task.

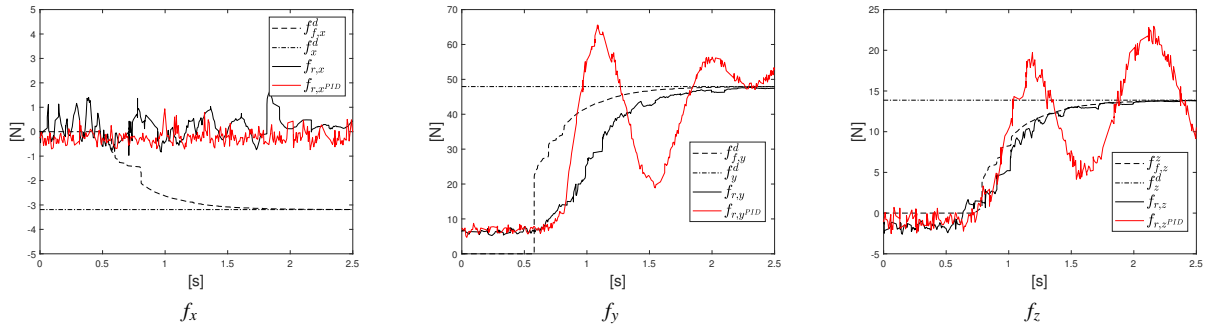

Fig. 6: Reference force $\mathbf{f}^d$ (dash-dot black line), filtered reference force $\mathbf{f}_f^d$ (dash black line), measured force $\mathbf{f}_r$ (continuous black line) from the use of the proposed force controller, and measured force $\mathbf{f}_{r^{PID}}$ (continuous red line) from the use of the constant-damping impedance controller with non-saturated PI are shown for the grasping phase. Ten repetitions of the experiment have been performed.

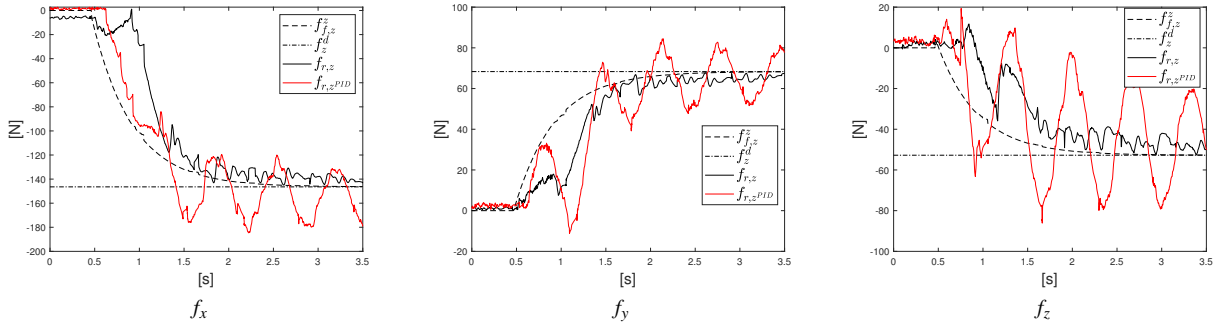

Fig. 7: Reference force $\mathbf{f}^d$ (dash-dot black line), filtered reference force $\mathbf{f}_f^d$ (dash black line), measured force $\mathbf{f}_r$ (continuous black line) from the use of the proposed force controller, and measured force $\mathbf{f}_{r^{PID}}$ (continuous red line) from the use of the constant-damping impedance controller with non-saturated PI are shown for the installation phase. Ten repetitions of the experiment have been performed.

Fig. 8: The assembly sub-tasks for the sidewall panel inside the aircraft cabin are shown, highlighting grasping and installation phases.

Reference force has been imposed equal to 50 N in the robot tool direction. Figure 6 shows the force-tracking capabilities of the proposed algorithm. The measured force $\mathbf{f}_r$ tracks the filtered reference force $\mathbf{f}_f^d$ and no overshoots are shown w.r.t. the step reference force $\mathbf{f}^d$. The standard controller, instead, shows force overshoots and instabilities. Considering installation phase, on the basis of the identified installation location, the robot is positioned to start the installation task. Reference force has been imposed equal to 170 N in the robot tool direction. Figure 7 shows the force-tracking capabilities of the proposed algorithm. The measured force $\mathbf{f}_r$ tracks the filtered reference force $\mathbf{f}_f^d$ and no overshoots are shown w.r.t. the step reference force $\mathbf{f}^d$. The standard controller, instead, shows force overshoots and instabilities. The complete assembly task is shown in Figure 8.

IV. Conclusions

The paper describes a control framework to enhance autonomous force-tracking tasks in industrial applications. Being composed by a 6D pose estimation system and by a variable damping impedance control with adaptive saturation PI force-controller, the proposed methodology allows to compensate for positioning and interaction dynamics uncertainties. Improved performance in both the 6D pose estimation of the part and in the force-tracking are shown in an assembly task of a sidewall panel in the aerospace industry. Future work aims to include the online estimation of the environment properties (*e.g.*, stiffness) to online optimize the control gains. AI techniques are also under development to recognize installation phases and task failures from force data, allowing the robot to correct the task.

REFERENCES

[1] M. Rüßmann, M. Lorenz, P. Gerbert, M. Waldner, J. Justus, P. Engel, and M. Harnisch, "Industry 4.0: The future of productivity and growth in manufacturing industries," *Boston Consulting Group*, vol. 9, 2015.

[2] S. Pfeiffer, "Robots, industry 4.0 and humans, or why assembly work is more than routine work," *Societies*, vol. 6, no. 2, p. 16, 2016.

[3] K.-D. Thoben, S. Wiesner, and T. Wuest, "Industrie 4.0 and smart manufacturing–a review of research issues and application examples," *Int. J. Autom. Technol*, vol. 11, no. 1, 2017.

[4] C. C. Kemp, A. Edsinger, and E. Torres-Jara, "Challenges for robot manipulation in human environments [grand challenges of robotics]," *IEEE Robotics & Automation Magazine*, vol. 14, no. 1, pp. 20–29, 2007.

[5] M. Mabkhot, A. Al-Ahmari, B. Salah, and H. Alkhalefah, "Requirements of the smart factory system: A survey and perspective," *Machines*, vol. 6, no. 2, p. 23, 2018.

[6] H. Bay, A. Ess, T. Tuytelaars, and L. Van Gool, "Speeded-up robust features (surf)," *Computer vision and image understanding*, vol. 110, no. 3, pp. 346–359, 2008.

[7] D. G. Lowe, "Distinctive image features from scale-invariant keypoints," *International journal of computer vision*, vol. 60, no. 2, pp. 91–110, 2004.

[8] S. Savarese and L. Fei-Fei, "3d generic object categorization, localization and pose estimation," in *2007 IEEE 11th International Conference on Computer Vision*. IEEE, 2007, pp. 1–8.

[9] M. Imperoli and A. Pretto, "D^2CO: Fast and robust registration of 3d textureless objects using the directional chamfer distance," in *International conference on computer vision systems*. Springer, 2015, pp. 316–328.

[10] C. Choi and H. I. Christensen, "3d textureless object detection and tracking: An edge-based approach," in *2012 IEEE/RSJ International Conference on Intelligent Robots and Systems*. IEEE, 2012, pp. 3877–3884.

[11] S. Hinterstoisser, V. Lepetit, S. Ilic, P. Fua, and N. Navab, "Dominant orientation templates for real-time detection of texture-less objects," in *2010 IEEE Computer Society Conference on Computer Vision and Pattern Recognition*. IEEE, 2010, pp. 2257–2264.

[12] A. Aldoma, M. Vincze, N. Blodow, D. Gossow, S. Gedikli, R. B. Rusu, and G. Bradski, "Cad-model recognition and 6dof pose estimation using 3d cues," in *2011 IEEE international conference on computer vision workshops (ICCV workshops)*. IEEE, 2011, pp. 585–592.

[13] A. Aldoma, Z.-C. Marton, F. Tombari, W. Wohlkinger, C. Potthast, B. Zeisl, R. B. Rusu, S. Gedikli, and M. Vincze, "Tutorial: Point cloud library: Three-dimensional object recognition and 6 dof pose estimation," *IEEE Robotics & Automation Magazine*, vol. 19, no. 3, pp. 80–91, 2012.

[14] W. Kehl, F. Manhardt, F. Tombari, S. Ilic, and N. Navab, "Ssd-6d: Making rgb-based 3d detection and 6d pose estimation great again," in *Proceedings of the IEEE International Conference on Computer Vision*, 2017, pp. 1521–1529.

[15] D. T. Le, M. Andulkar, W. Zou, J. P. Städter, and U. Berger, "Self adaptive system for flexible robot assembly operation," in *Emerging Technologies and Factory Automation (ETFA), 2016 IEEE 21st International Conference on*. IEEE, 2016, pp. 1–5.

[16] N. Hogan, "Impedance control: An approach to manipulation," in *American Control Conference, 1984*, june 1984, pp. 304–313.

[17] H. Seraji and R. Colbaugh, "Force tracking in impedance control," *The Int Journal of Robotics Research*, vol. 16, no. 1, pp. 97–117, 1997.

[18] X. Liang, H. Zhao, X. Li, and H. Ding, "Force tracking impedance control with unknown environment via an iterative learning algorithm," in *2018 3rd International Conference on Advanced Robotics and Mechatronics (ICARM)*. IEEE, 2018, pp. 158–164.

[19] S. S. M. Salehian and A. Billard, "A dynamical system based approach for controlling robotic manipulators during non-contact/contact transitions," *IEEE Robotics and Automation Letters*, 2018.

[20] J. Buchli, F. Stulp, E. Theodorou, and S. Schaal, "Learning variable impedance control," *The International Journal of Robotics Research*, vol. 30, no. 7, pp. 820–833, 2011.

[21] G. J. Lahr, H. B. Garcia, J. O. Savazzi, C. B. Moretti, R. V. Aroca, L. M. Pedro, G. F. Barbosa, and G. A. Caurin, "Adjustable interaction control using genetic algorithm for enhanced coupled dynamics in tool-part contact," in *Intelligent Robots and Systems (IROS), 2017 IEEE/RSJ International Conference on*. IEEE, 2017, pp. 1630–1635.

[22] J. Duan, Y. Gan, M. Chen, and X. Dai, "Adaptive variable impedance control for dynamic contact force tracking in uncertain environment," *Robotics and Autonomous Systems*, vol. 102, pp. 54–65, 2018.

[23] E. Shahriari, A. Kramberger, A. Gams, A. Ude, and S. Haddadin, "Adapting to contacts: Energy tanks and task energy for passivity-based dynamic movement primitives," in *2017 IEEE-RAS 17th International Conference on Humanoid Robotics (Humanoids)*. IEEE, 2017, pp. 136–142.

[24] K. M. El Dine, J.-A. Corrales-Ramon, Y. Mezouar, and J.-C. Fauroux, "A smooth position-force controller for asbestos removal manipulator," in *2017 IEEE International Conference on Robotics and Biomimetics (ROBIO)*. IEEE, 2017, pp. 1312–1319.

[25] L. Roveda, N. Iannacci, F. Vicentini, N. Pedrocchi, F. Braghin, and L. Molinari Tosatti, "Optimal impedance force-tracking control design with impact formulation for interaction tasks," *IEEE Robotics and Automation Letters*, vol. 1, no. 1, pp. 130–136, 2016.

[26] W.-C. Chang, "Robotic assembly of smartphone back shells with eye-in-hand visual servoing," *Robotics and Computer-Integrated Manufacturing*, vol. 50, pp. 102–113, 2018.

[27] C. Cai and N. Somani, "Visual servoing in a prioritized constraint-based torque control framework," in *2018 IEEE/ACIS 17th International Conference on Computer and Information Science (ICIS)*. IEEE, 2018, pp. 309–314.

[28] Y. Ma, K. Du, D. Zhou, J. Zhang, X. Liu, and D. Xu, "Automatic precision robot assembly system with microscopic vision and force sensor," *International Journal of Advanced Robotic Systems*, vol. 16, no. 3, p. 1729881419851619, 2019.

[29] L. Roveda, S. Ghidoni, S. Cotecchia, E. Pagello, and N. Pedrocchi, "EURECA H2020 CleanSky 2: a multi-robot framework to enhance the fourth industrial revolution in the aerospace industry," in *2017 IEEE International Conference on Robotics and Automation (ICRA), Workshop on Industry of the future: Collaborative, Connected, Cognitive. Novel approaches stemming from Factory of the Future and Industry 4.0 initiatives*, 2017.

[30] R. B. Rusu, Z. C. Marton, N. Blodow, M. Dolha, and M. Beetz, "Towards 3d point cloud based object maps for household environments," *Robotics and Autonomous Systems*, vol. 56, no. 11, pp. 927–941, 2008.

[31] T. Rabbani, F. Van Den Heuvel, and G. Vosselmann, "Segmentation of point clouds using smoothness constraint," *International archives of photogrammetry, remote sensing and spatial information sciences*, vol. 36, no. 5, pp. 248–253, 2006.

[32] P. J. Besl and N. D. McKay, "Method for registration of 3-d shapes," in *Sensor Fusion IV: Control Paradigms and Data Structures*, vol. 1611. International Society for Optics and Photonics, 1992, pp. 586–607.

[33] W. Chung, I. Kim, and J. Joh, "Null-space dynamics-based control of redundant manipulators in reducing impact," *Control Engineering Practice*, vol. 5, no. 9, pp. 1273–1282, 1997.

[34] S. Zennaro, M. Munaro, S. Milani, P. Zanuttigh, A. Bernardi, S. Ghidoni, and E. Menegatti, "Performance evaluation of the 1st and 2nd generation kinect for multimedia applications," in *Multimedia and Expo (ICME), 2015 IEEE International Conference on*. IEEE, 2015, pp. 1–6.

[35] E. Olson, "AprilTag: A robust and flexible visual fiducial system," in *Proceedings of the IEEE International Conference on Robotics and Automation (ICRA)*. IEEE, May 2011, pp. 3400–3407.

[36] R. Y. Tsai and R. K. Lenz, "A new technique for fully autonomous and efficient 3d robotics hand/eye calibration," *IEEE Transactions on robotics and automation*, vol. 5, no. 3, pp. 345–358, 1989.